Semiquantitative Analysis of Hypothalamic Damage on MRI Predicts Risk for Hypothalamic Obesity

Christian L. Roth[1,2], Hedieh Eslamy[3], David Werny[2], Clinton Elfers[1], Michele L. Shaffer[4], Catherine Pihoker[2], Jeffrey Ojemann[5], and William B. Dobyns[1]

Objective: Excessive weight gain frequently occurs in patients with hypothalamic tumors and lesions leading to hypothalamic obesity (HO).

Methods: Digital brain magnetic resonance imaging (MRI) and clinical outcomes were studied retrospectively in a single center, including 45 children with postoperative lesions in the sellar region (41 craniopharyngiomas, 4 with Rathke's cleft cysts), $\sim$5 years post-surgery, mean age 13.9 years. Four standard sections covering hypothalamic areas critical to energy homeostasis were used to assess lesions and calculate a hypothalamic lesion score (HLS); the association with HO was examined.

Results: Compared to subjects who did not develop HO ($n = 23$), subjects with HO ($n = 22$) showed more frequently lesions affecting the third ventricular floor, mammillary bodies, and anterior, medial (all $P < 0.05$), and most importantly posterior hypothalamus ($P < 0.01$). The HLS correlated significantly with BMI z-score changes 12 and 30 months post-surgery, even after adjusting for potential confounders of gender, age at surgery, surgery date, surgery BMI z-score, hydrocephalus, and residual hypothalamic tumor ($r = 0.34$, $P = 0.03$; $r = 0.40$, $P = 0.02$, respectively). Diabetes insipidus was found to be an endocrine marker for HO risk.

Conclusions: The extent of damage following surgery in the sellar region can be assessed by MRI using a novel scoring system for early HO risk assessment.

Introduction

Excessive weight gain and its resultant cardiometabolic abnormalities frequently occur in patients with tumors in the hypothalamic region leading to hypothalamic obesity (HO). Most tumors in this region are craniopharyngiomas (CPs), the most common suprasellar tumors of non-glial origin in children (1,2). Rathke's cleft cysts (RCCs) are benign lesions of the pituitary region, which can be asymptomatic (3) and are frequently detected during autopsies. Symptomatic RCCs are rare and can cause headaches, visual impairment, and pituitary hormone deficiencies. CPs and RCCs are closely related and may be part of a continuum of ectodermally derived epithelial lesions (4,5).

The treatment of choice for both CP and symptomatic RCC is gross total resection or less radical surgery in combination with radiotherapy to preserve optic nerve and hypothalamic structures and minimize other complications (6,7). Postsurgical CP patients experience increased rates of obesity, which is a major contributor to CP-related morbidity and

mortality (8). Prediction, prevention, and early initiation of obesity treatment are vital to decrease the rate of cardiovascular disease, because HO is more resistant to treatment than common obesity (9-13).

Despite previous neuroimaging studies (14-16), the mechanisms by which damage to the hypothalamus leads to more or less severe forms of obesity are still unclear. Here we assess the relationship between HO development and hypothalamic damage using standard postoperative brain imaging. We show that post-surgery BMI data correlated significantly with our newly developed hypothalamic lesion score (HLS) and that lesions which include the posterior hypothalamus are associated with a very high risk for HO development.

Methods

Patients

The study was approved by the Seattle Children's Hospital Institutional Review Board. Clinical data including brain imaging studies

[1] Center for Integrative Brain Research, Seattle Children's Hospital & Research Institute, Seattle, Washington, USA. Correspondence: Christian L. Roth (christian.roth@seattlechildrens.org) [2] Pediatric Endocrinology, Seattle Children's Hospital & Research Institute, Seattle, Washington, USA [3] Neuroradiology, Seattle Children's Hospital & Research Institute, Seattle, Washington, USA [4] Center for Clinical and Translational Research, Seattle Children's Hospital & Research Institute, Seattle, Washington, USA [5] Neurosurgery, Seattle Children's Hospital & Research Institute, Seattle, Washington, USA

and outcomes were analyzed retrospectively. From a total of 56 patients who had surgery for CP ($n = 51$) or RCC ($n = 5$) at Seattle Children's Hospital from 1996 to 2013, 45 children and adolescents (41 with CP and 4 with RCC; 22 males and 23 females) fulfilled the inclusion criteria as all had documented clinical data and electronically stored brain magnetic resonance imaging (MRI) studies available for scoring, while 11 subjects were excluded because MRIs were not available. Surgery was performed at age 8.4 ± 4.0 years by transcranial ($n = 35$) or transsphenoidal ($n = 10$) approach. Additionally, 29 subjects underwent transcranial irradiation (of which 8 received proton beam irradiation) because of incomplete resection of the tumor or tumor recurrence. Subjects' BMI and BMI z-scores were assessed at time of surgery and at last visit (age 13.9 ± 4.5 years; 5.5 ± 4.5 years after surgery). In a subset of patients, BMI and BMI z-scores also could be assessed at 12 (11.5 ± 3.5 months, 39 subjects) and 30 (30.3 ± 7.5 months, 36 subjects) months following surgery. Last visit BMI z-scores were used to classify patients who developed HO (group HO, $n = 22$) versus patients without HO (group No-HO, $n = 23$; see Table 1). Subjects were assigned to the HO group if they (1) were obese at time of last visit (BMI exceeding the 95th percentile using CDC charts), and (2) showed significant increase in BMI (ΔBMI z-score ≥ 0.25 during first 6 months following surgery) post-surgery or directly before surgery (within 1 year before surgery) in order to differentiate HO from common obesity. Except for one patient with CP and one with RCC, patients received perioperative dexamethasone treatment for 2-12 days. The most frequent starting dose was 4 mg every 6 h or in younger patients 2 mg every 6 h, with dose and frequency tapered over several days. All patients were on hormonal replacement as required, except for 5 of 26 growth hormone (GH) -deficient subjects who were not supplemented with GH (Table 1).

Neuroradiological imaging

Brain images were retrospectively assessed using electronically stored T1 weighed MRI data 1.9 ± 2.8 years following surgery (at 10.2 ± 4.1 years). We aimed to score brain images that were performed shortly after surgery but at least 3 months past surgery to avoid misinterpretations due to acute postoperative changes such as blood remains and inflammation. In subjects whose brain imaging was performed several years after surgery, we checked that no additional surgery was performed. Lesion scores were assessed in four standard T1 weighed images (see overview in Figure 1.1 and examples in Figure 1.2): (a) midsagittal section (Figure 1.2 A,E,I,M), (b) coronal section through the anterior commissure (Figure 1.2 B,F,J,N), (c) coronal section midway between the anterior commissure and mammillary bodies [+5.4 mm posterior from anterior commissure according to Mai et al. (17), see Figure 1.2 C,G,K,O], and (d) coronal section through the mammillary bodies [+10.7 mm posterior from anterior commissure (17), see Figure 1.2 D,H] or through the basilar artery coursing caudo-cranially and anterior to the pons if the mammillary bodies are damaged (e.g., Figure 1.2 L,P). This allowed us to assess damage in different hypothalamic areas and relate it to specific brain nuclei that are critically involved in energy homeostasis. The four brain sections assessed included: the floor of the third ventricle which contains the arcuate nucleus (ARC); pituitary and pituitary stalk (section a); anterior hypothalamus including paraventricular nucleus (PVN, section b); medial hypothalamus containing the ARC and ventromedial nucleus (VMN, section c); and mammillary bodies/posterior hypothalamus containing the dorsomedial nucleus (DMN) and dorsal hypothalamic area (DHA; section d).

In addition, third and lateral ventriculomegaly as well as residual hypothalamic tumor were assessed (Figure 1.2, sections b-d). The coordinates and shapes for different brain nuclei were based on the Atlas of the Human Brain (17), as well as previous publications in this field (18-20). Individual brain structures were scored as 0 (intact) or 1 (deficient, abnormal) and bilateral structures as 0 (intact), 0.5 (unilateral damage), or 1 (bilateral damage), as summarized in Supporting Information Table 1. Neuroimaging scoring was performed by three physicians (CLR, HE, WBD), including a neuroradiologist (HE) who was blinded for the clinical outcomes. Agreement of at least two of the three investigators was necessary for final scoring. The presence of hydrocephalus or residual tumor (no: 0; yes: 1) was used as an adjustment variable in correlation analyses as this could distort the location of the target brain structures.

Statistical analysis

BMI z-scores were calculated as a normalized measurement for the severity of obesity using the LMS method (21). Analysis of lesion scores was performed in two steps. First we compared all 11 criteria (see criteria for damaged regions in Table 2) in two groups, HO versus No-HO at last appointment. Second we selected the criteria that achieved at least marginally significant differences between groups (defined by $P < 0.1$) in order to create a HLS (Supporting Information Table 1). This score was used for further correlation analyses regarding postoperative BMI z-score changes and for BMI analyses in groups with different types of lesions.

Diagnostic histograms were prepared for all continuous variables to assess approximate normality, which was confirmed for all the studied outcomes. For two group comparisons (HO vs. No-HO) of continuous variables with approximately normal distributions, Student's t-test was used for unpaired observations and paired Student's t-test for paired observations as normality assumptions were not violated. For two group comparisons of categorical variables for unpaired observations, Fisher's exact test was used. Multiple group comparisons were performed by analysis of variance followed by Bonferroni post-hoc testing for pairwise comparisons (Prism® program, GraphPad Software, San Diego, CA). Pearson correlation coefficients were used to examine correlations between the lesion score and clinical outcome variables. Partial Pearson correlation coefficients were used to adjust for potential covariates such as gender and age at surgery, as both could be related to BMI, BMI z-score at time of surgery, and date of surgery as surgical techniques potentially could have changed over the time of this study, as well as presence of residual tumor and hydrocephalus, as this could distort the location of the target brain structures. Correlation analyses were conducted using SAS Version 9.2 (SAS Institute, Cary, NC). Data are shown as mean ± SD in text and tables, or as means and standard errors as well as correlation coefficients (r) in figures. All differences were considered significant for P-values less than 0.05 using two-tailed tests.

Results

Using electronically stored MRIs of moderate imaging quality, we were able to assess the extent and location of damage in specific brain regions in 45 subjects post-surgery (Figure 1 and Supporting Information Figure 1). In a subset of 24 subjects, we also were able to score MRIs obtained within 1 month before surgery. Comparing HLS results of these 24 subjects from pre- versus post-

TABLE 1 Descriptive data and hormone supplementation in 45 subjects with and without development of HO

	No-HO	HO	*P*-value
Number of subjects (male/female)	23 (11/12)	22 (11/11)	
Type of tumor (CP/RCC)	21/2	20/2	
Last visit BMI (kg/m^2)/BMI *z*-score	21.1/0.36	34.1/2.27	
Surgery BMI (kg/m^2)/BMI *z*-score	17.2/0.01	21.6/1.38	0.0374/0.0003[a]
Age last visit/years after surgery (years)	13.7/4.7	14.1/6.5	0.772/0.179[a]
Incomplete resection, *n* (% per group)	19 (83)	12 (54)	0.057[b]
Evidence for recurrence, *n* (% per group)	10 (43)	7 (32)	0.542[b]
Cranial irradiation, *n* (% per group)	15 (65)[c]	14 (64)[d]	1[b]
Cumulative perioperative dexamethasone, mg (SD)	55.2 (29.8)	53.8 (38.2)	0.919[a]
DDAVP, *n* (% per group)	9 (39)	18 (82)	0.006[b]
Hydrocortisone, *n* (% per group)	15 (65)	20 (91)	0.071[b]
Gonadal steroids, *n* (% per group)	4 (17)	1 (5)	0.346[b]
GH, *n* (% per group)	12 (52)[e]	9 (41)[f]	0.554[b]
Thyroid hormone, *n* (% per group)	18 (78)	20 (91)	0.414[b]

[a]*P*-value by Student's *t*-test.
[b]*P*-value by Fisher's exact test.
[c]Received proton beam irradiation among irradiated subjects, *n* = 6.
[d]Received proton beam irradiation among irradiated subjects, *n* = 2.
[e]Additional GH-deficient subjects, but no GH supplementation, *n* = 4.
[f]Additional GH-deficient subjects, but no GH supplementation, *n* = 1.

surgery scans (example in Supporting Information Figure 2), we found better correlations for HO development using the post-surgery scans, although we found that both scores were correlated significantly ($r = 0.74$, $P < 0.0001$). In these 24 subjects, pre-surgery HLS correlated similarly significantly with changes of the BMI *z*-score at 12 and 30 months following surgery, similarly to post-surgery HLS ($P < 0.01$ for all comparisons). However, only post-surgery HLS correlated significantly with BMI *z*-scores at last

TABLE 2 Neuroimaging scoring of hypothalamic lesion in relation to topographic region

Assessment of	Brain Section	Subjects without HO, *n* (%)	Subjects with HO, *n* (%)	*P*-value
1. Pituitary lesion	a) Midsagittal	20 (87)	22 (100)	0.2333
2. Pituitary stalk lesion	a) Midsagittal	20 (87)	19 (86)	0.6078
3. Floor of the third ventricle (ARC)	a) Midsagittal	10 (43)	18 (82)	**0.0134**
4. Anterior hypothalamus (PVN)	b) Coronal through anterior commissure	10 (43)	19 (86)	**0.0045**
5. Medial hypothalamus (VMN, ARC)	c) Coronal between anterior commissure and mammillary bodies	9 (39)	19 (86)	**0.0018**
6. Posterior hypothalamus (DMN, DHA)	d) Coronal through mammillary bodies	4 (17)	10 (45)	**<0.0001**
7. Mammillary bodies	d) Coronal through mammillary bodies	3 (13)	15 (68)	**0.0002**
8. Third ventriculomegaly	b-d	8 (35)	16 (73)	**0.0169**
9. Lateral ventriculomegaly	b-d	3 (13)	11 (50)	**0.0106**
10. Residual suprasellar Tu	b-d	15 (65)	11 (50)	0.2362
11. Residual hypothalamic Tu	b-d	8 (35)	9 (41)	0.7631

P-values based on Fisher's exact test (HO vs. No-HO) comparing two groups of scores (intact: 0; damaged: 0.5 or 1). Criteria 3-9 were also used in HLS (gray box, significant *P*-values in bold letters). The posterior hypothalamic section showed the strongest differences between the groups (dark gray).
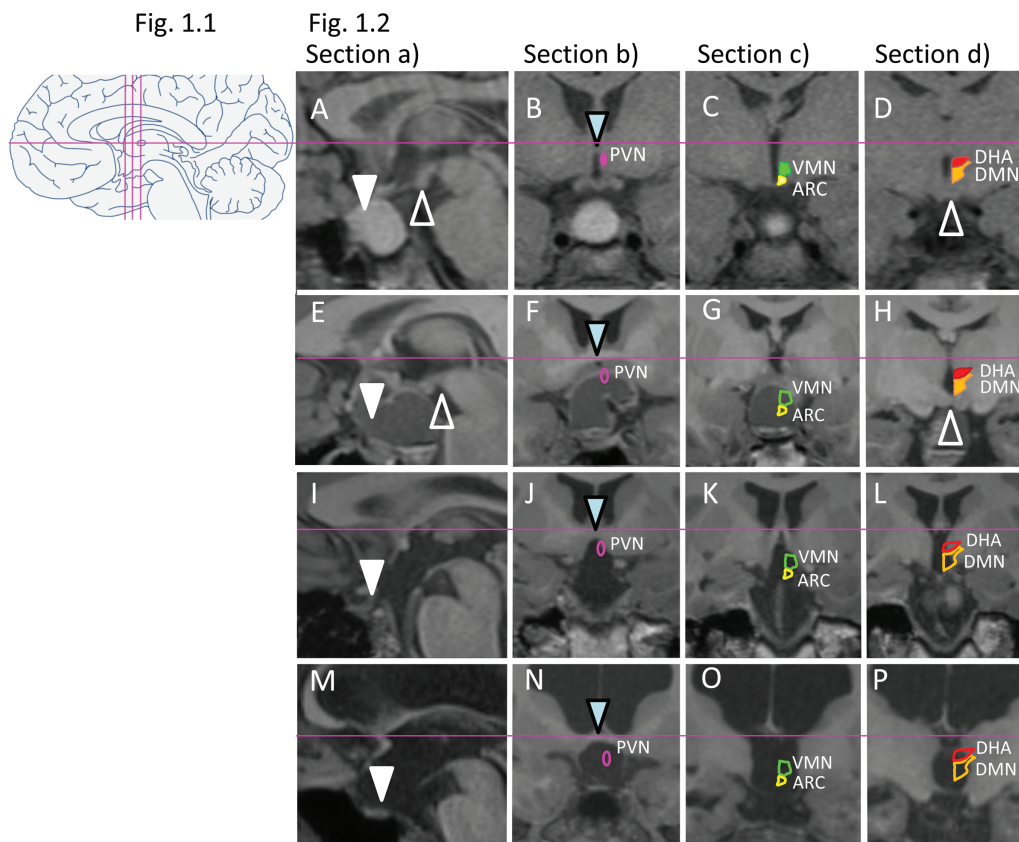
Figure 1 1.1: Schematic overview of standard brain sections for assessment of lesions (midline sagittal: a; three coronal sections: b, c, d). 1.2: MRI standard brain sections and HLS in four patients following craniopharyngioma resection. Solid shapes of nuclei indicate intact structures, while open shapes indicate lesions. **A-D**: Male patient presenting with residual intra-/suprasellar tumor (A), while PVN (pink in B), ARC (yellow in C), and VMN (green in C), as well as DHA (red in D) and DMN (orange in D), are still intact. HLS: 0. BMI z-score at surgery -1.11 (age 11 years), BMI z-score 3 years post-surgery -0.6. (**E-H**): Female patient showing a residual suprasellar/hypothalamic cystic lesion and defect of the anterior and medial hypothalamus. HLS: 3. BMI z-score at surgery 0.09 (age 14 years), BMI z-score 2 years post-surgery 0.13. (**I-L**): Female patient with BMI z-score at surgery 2.22 (age 7 years) presenting with large postoperative lesion affecting the floor of the third ventricle and whole hypothalamus. HLS: 5. BMI z-score 3 years post-surgery 2.28. (**M-P**): Female patient presenting with large lesion, hydrocephalus, and absence of pituitary, optic chiasm, pituitary stalk, floor of third ventricle, PVN, ARC, VMN, DHA, and DMN. HLS: 7. BMI z-score at surgery 0.71 (age 11 years), BMI z-score 2 years post-surgery 1.87. Triangles point to landmarks of orientation: sella (white), mammillary bodies (white open), and anterior commissure (blue).

visit ($r = 0.627$, $P = 0.001$ vs. $r = 0.358$, $P = 0.086$ for pre-surgery HLS). With this in mind and also because of the larger dataset we focused our subsequent analysis on post-surgery imaging results.

Comparison of two groups, patients with versus without HO

First we investigated clinical variables in two groups of subjects according to their BMI at the time of their last visit. Twenty-two of the 45 evaluated patients had HO at their last visit (average 66 months following surgery). These subjects already had significantly higher BMI z-scores at the time of surgery (Table 1). Both groups (HO and No-HO) increased their BMI z-scores significantly during the first year following surgery, but no additional gains in BMI z-scores were seen after the first year (Figure 2A). As not all BMI assessments occurred precisely at 12 or 30 months after surgery, we

also calculated changes of BMI z-scores per month, which confirmed the findings (Figure 2B). Recurrence and cranial irradiation rates were comparable in both groups, while there was a non-significant trend toward a higher rate of incomplete resections in the No-HO group (Table 1). The cumulative perioperative dexamethasone dose did not differ between groups, and there was no association between cumulative perioperative dexamethasone dose and delta BMI z-score during 12 months ($r = 0.152$, $P = 0.447$) or 30 months ($r = 0.124$, $P = 0.581$) following surgery. We used hormonal supplementation as a surrogate for hormonal deficiencies. There were no significant differences between the two groups except for desmopressin, a surrogate for diabetes insipidus (DI), which was more frequent in the HO versus the No-HO group (Table 1).

Second, we investigated differences in postsurgical brain imaging in HO versus No-HO groups of subjects. Lesions in the anterior,
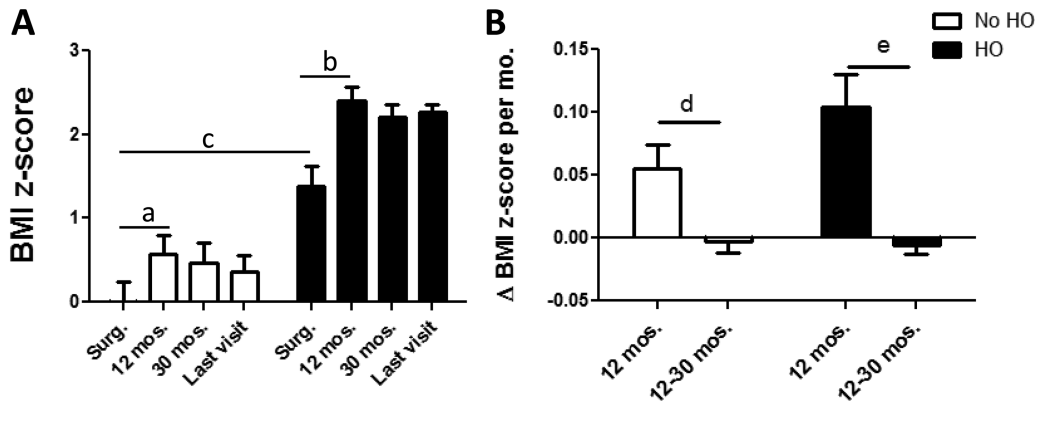
Figure 2 BMI *z*-scores at time of surgery (Surg.), 12 (11.5 ± 3.5) and 30 (30.3 ± 7.5) months following surgery, and at last visit (average 66 months post-surgery) in patients with (black bars) versus without (white bars) HO development (*P* = 0.0003 at time of surgery). (**A**) In both groups, BMI *z*-scores increased significantly 12 months following surgery ([a]*P* = 0.016/[b]*P* = 0.0007, paired *t*-test). At time of surgery, BMI *z*-scores were already significantly different in the HO versus the No-HO group ([c]*P* = 0.0003, Student's *t*-test). (**B**) Strong changes of BMI *z*-scores per month were seen in both groups 12 months post-surgery but no further changes during the subsequent period 12-30 months post-surgery ([d]*P* = 0.0147/[e]*P* = 0.0002, Student's *t*-test).

medial, and posterior hypothalamus, as well as floor of the third ventricle and mammillary bodies, were more frequent in the HO versus the No-HO group (Table 2). In order to create the HLS, we selected the criteria that achieved at least marginal significance between both groups, which resulted in a selection of seven out of 11 tested criteria (using criteria 1-7 in Table 2; Supporting Information Table 1). The HLS was significantly higher in patients with HO versus No-HO (5.3 ± 2.3 vs. 2.2 ± 2.3, *P* = 0.0003). From a Pearson correlation analyses, the HLS correlated significantly with changes of the BMI *z*-score at 12 months (*r* = 0.515, *P* = 0.0007) and 30 months (*r* = 0.447, *P* = 0.0062) following surgery (Figure 3A,B), even when adjusted for potential confounders including gender, age at surgery, hydrocephalus, residual hypothalamic tumor,

BMI *z*-score at time of surgery, and date of surgery (*r* = 0.508, *P* = 0.0021; *r* = 0.559, *P* = 0.0013, respectively).

Comparison of outcomes related to the extent of lesions

As a third step, changes in BMI in three groups of subjects separated by the sites of lesions were analyzed using the same data: subjects without evidence of any hypothalamic lesions (No HL) versus subjects with lesions of the anterior and/or medial hypothalamus (AM) versus subjects with lesions in the anterior and/or medial hypothalamus plus the posterior hypothalamus (AM + P), as all of the patients with damage in the posterior hypothalamus also showed damage to the anterior
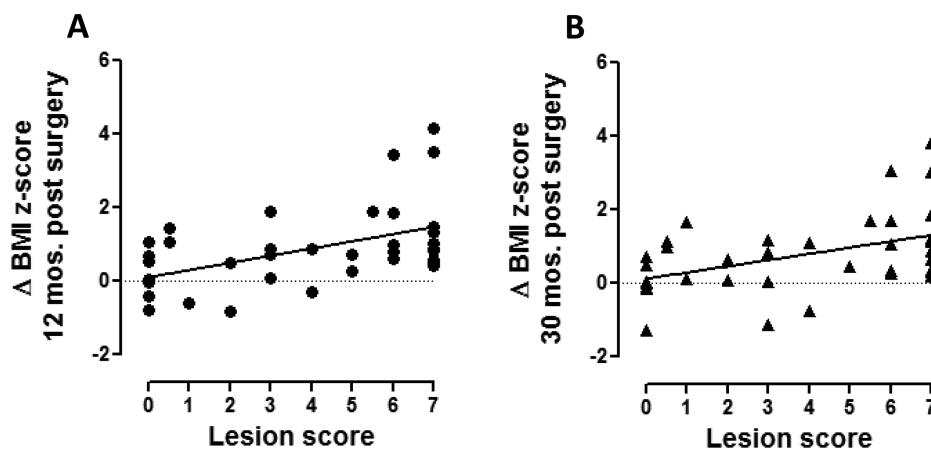

Figure 3 Relationship between HLS and postoperative change of BMI *z*-scores. Correlation analyses investigating the relationship between the HLS and change of BMI *z*-score (**A**) 12 months and (**B**) 30 months post-surgery Pearson correlation *r* = 0.515, *P* = 0.0007 at 12 months and *r* = 0.447, *P* = 0.0062 at 30 months following surgery.
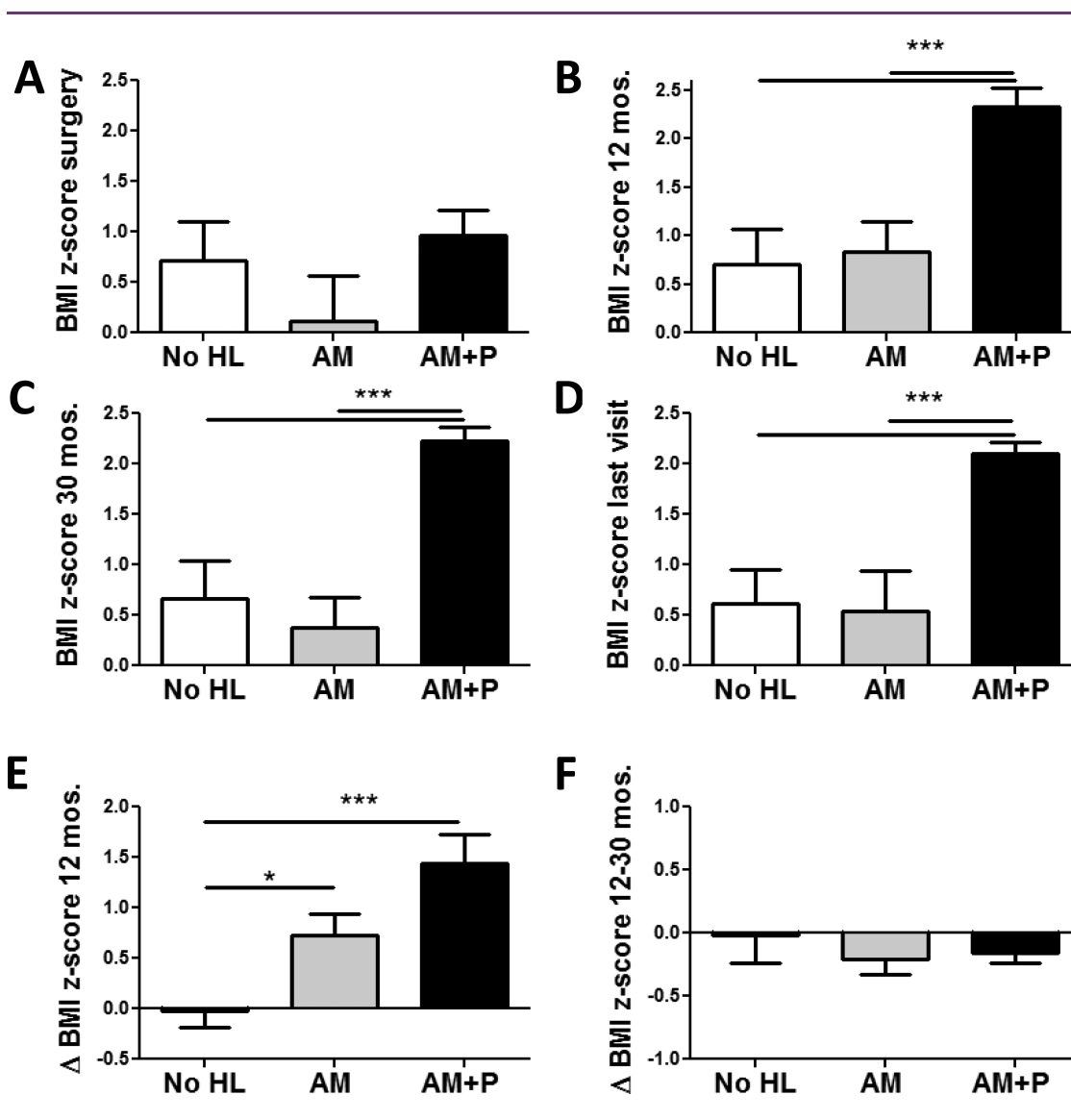
Figure 4 Changes of BMI *z*-scores in relation to extent of lesion. BMI *z*-scores in patients without hypothalamic lesions (No HL, white bars), lesions of the anterior and/or medial hypothalamus (AM, gray bars), or lesions in the posterior hypothalamus as well as in the anterior and/or medial hypothalamus (AM + P, black bars). BMI *z*-scores (**A**) at time of surgery, and at (**B**) 12 and (**C**) 30 months later as well as (**D**) at last visit. Changes of BMI *z*-scores (**E**) from surgery to 12 months and (**F**) from 12 to 30 months post-surgery. *$P < 0.05$ and ***$P < 0.001$.

and/or medial hypothalamus. Although there were no significant differences of BMI *z*-scores at time of surgery (Figure 4A), the AM + P group showed the strongest postoperative weight gains during the first 12 months following surgery, resulting in significantly higher BMI *z*-scores 12 and 30 months following surgery as well as at last visit (Figure 4B-F). The HLS for each group was 0 (no HL), 2.60 ± 1.24 (group AM), and 6.38 ± 0.78 (group AM + P).

Testing DI as an endocrine marker for HO development

Finally, we tested presence of postsurgical DI as an easily accessible endocrine marker for HO risk. Comparing patients with DI ($n = 27$) versus without DI ($n = 18$), subjects with DI had similar BMI *z*-scores

at surgery (0.69 ± 1.23 vs. 0.65 ± 1.32, $P = 0.919$). However, their postoperative BMI changes were significantly greater at 12 months (delta BMI *z*-score 1.10 ± 1.20 vs. 0.37 ± 0.68, $P = 0.034$) and 30 months (delta BMI *z*-score 1.77 ± 1.10 vs. 0.30 ± 0.78, $P = 0.035$) post-surgery, resulting in a higher rate of HO at last visit (17/27 vs. 5/18, $P = 0.033$). In addition, DI subjects showed more frequent lesions in the medial (81 vs. 44%, $P = 0.022$) and especially posterior (74 vs. 6%, $P < 0.0001$) hypothalamus, but only a non-significant trend for the anterior hypothalamus (78 vs. 50%, $P = 0.105$).

Discussion

This study describes development of a novel MRI scoring system to quantify hypothalamic damage following surgery in the hypothalamic-

pituitary region which allows postoperative risk assessment for HO development. To our knowledge, this is the first neuroimaging scoring system that directly relates brain images showing lesions affecting different hypothalamic areas to specific brain nuclei critically involved in energy homeostasis. Our data clearly demonstrate that patients with postoperative lesions that include the DHA and DMN in the posterior hypothalamus are at very high risk for rapid and pathological weight gain during the first year following surgery [sometimes beginning in the months prior to surgery (1,22)], and that damage to this region is a reasonably good surrogate for the HLS in CP and RCC subjects. In contrast to a previous study (23), we found no correlation between perioperative dexamethasone doses and weight gain during the first year following CP surgery.

Our approach builds on the prior work of different groups (10,11,14-16,24). An advantage of our HLS system is that it assesses lesions using anatomical landmarks in both sagittal and several coronal planes, and does not require measurements or volume assessments, which are often difficult to compare between subjects. Previous studies included measurements of the two- or three-dimensional assessments of hypothalamic damage and compression (24-26). However, as the whole human hypothalamus has a volume of only 4 ml (10), and is thereby much smaller than many of the CP tumors before surgery, we decided to assess damage to distinct areas that contain key neurons of energy homeostasis.

The HLS system can be used even in subjects with incomplete resection of the tumor. We believe that the HLS system is suitable for use in multicenter studies, as it requires only T1 weighed standard sagittal and coronal sections through the hypothalamic area and it can be applied effectively even with mildly suboptimal (fair to good) images. Our data also show that presence or absence of damage to the posterior hypothalamus is by itself a reliable predictor of HO. However, we believe that use of the complete HLS system is preferable because it examines more structures and should be applicable to other structural lesions of this region than CP and RCC.

In this study, about one half of patients developed HO, which is similar to previous studies (1,22). In comparison to subjects without HO, patients who developed HO already had a higher BMI at surgery and had a stronger postsurgical gain in BMI. Their lesions more frequently involved the anterior, medial and particularly posterior hypothalamus, as well as floor of the third ventricle and mammillary bodies (Table 2). This is in line with prior studies, which showed the association between large structural defects of the medial hypothalamus and development of severe obesity postsurgery (16,24,25,27,28). However, another study did not find this relationship (29). Recently, Muller et al. (14) reported that location and size of the hypothalamic lesion is associated with development of HO as patients with large lesions reaching the posterior hypothalamus and mammillary bodies had large increases in BMI. However, previous studies did not specifically evaluate damage in different nuclei involved in body weight regulation. In our study, we included the three hypothalamic sections that contain key nuclei regulating metabolism, as well as the mammillary bodies, structures which are important for memory function (30) and can easily be recognized as structural landmarks in close proximity to posterior hypothalamic nuclei. In addition, we also considered whether damage to bilateral nuclei was unilateral or bilateral, as intact contralateral pathways could potentially compensate for deficient neurons and neuronal projections.

Our observation of a very high risk for HO in patients with lesions that include the posterior hypothalamus fits well with the anatomical substrates of energy homeostasis, as distinct but overlapping neuronal pathways regulate various aspects of feeding behavior (31). Key regions are dispersed throughout the hypothalamus with important centers located in anterior (PVN), middle (ARC, VMN), and posterior (DMN, DHA) regions. The ARC contains two well-studied neuronal populations (31), one expressing proopiomelanocortin (POMC), a precursor of α-melanocyte stimulating hormone that inhibits food intake and stimulates energy expenditure; the other coexpressing agouti-related peptide and neuropeptide-Y, which of both stimulate food intake and reduce energy expenditure. ARC neurons project to several brain areas of energy regulation, including the PVN, lateral hypothalamus, and dorsal hypothalamic nuclei (32). The ARC expresses leptin receptors similar to the VMN and PVN (33). The DMN contains gamma-aminobutyric acid and neuropeptide-Y expressing neurons as well as α-melanocyte stimulating hormone terminals projecting from the ARC. DMN projections contribute to the stimulation of thyrotropin-releasing hormone neurons in the PVN (34). DMN, DHA, and VMN are key nuclei for locomotion and thermoregulation mediating leptin-induced sympathetic activation of brown adipose tissue and energy expenditure (35).

Disruption of feeding circuits by damage to the medial hypothalamic nuclei has the potential to increase hunger by unopposed activation of orexigens from the lateral hypothalamus, or by blocking the response to adiposity signals such as leptin and POMC in the medial hypothalamus. Thus, hypothalamic lesions have the potential to disrupt regulation of body weight and energy expenditure at many levels, finally resulting in a complex clinical picture of HO syndrome characterized by severe obesity associated with leptin resistance, fatigue, hyperphagia, impaired satiety, decreased sympathetic tone, and low energy expenditure (11,28,36-38). Our data suggest that several medial hypothalamic nuclei (PVN, ARC, VMN, DMN, DHA) must be damaged, similarly to findings in our previously established rodent model for lesion-induced HO, which demonstrates that only lesions affecting several medial hypothalamic nuclei (ARC, VMN, and DMN) resulted in the classical phenotype of HO described above (39).

Our study has several limitations. First, due to the retrospective nature of the study, it was challenging to obtain brain images within the first year after surgery from patients who had surgical procedures more than 10 years ago. Therefore, we used later MRIs as surrogates for the 3 months post-surgery MRI status. Second, in contrast to a recent study from Elowe-Gruau et al. (15), we focused on postoperative MRI, as pre-surgery scans were available only in about half of the studied subjects. In the subset for which pre- and post-surgery scans were available, we found that post-surgery imaging results correlated better with HO outcomes than pre-surgery imaging. Preoperative compression of the posterior hypothalamus that resolved post-surgically could explain this difference (Supporting Information Figure 2). Certainly future prospective studies should examine both preoperative and postoperative images to assess damage to the posterior hypothalamus.

Our data show that patients with DI and separately patients with HO are more likely to have lesions in the medial and posterior hypothalamus compared to patients without DI or HO. Thus, presence of DI serves as a prognostic marker for HO, and vice versa.

In summary, we have retrospectively assessed the extent of hypothalamic damage after surgeries in the sellar/suprasellar region using

standard MRI to identify anatomical landmarks in the pituitary-hypothalamic area, and correlated this with development of HO and DI. Future studies will show if the HLS system is suitable for early postoperative HO risk assessment, which is critical in order to prevent strong weight gain in particular during the first postoperative year. Extensive bilateral lesions affecting the posterior hypothalamus, which includes the DHA and DMN, were associated with the highest risk for HO development. Patients with lesions in this area need intensive multidisciplinary management by nutritional, psychological and endocrine care providers. Further options include bariatric surgery (40) and potentially available pharmacological interventions in the future. O

References

1. Muller HL, Emser A, Faldum A, et al. Longitudinal study on growth and body mass index before and after diagnosis of childhood craniopharyngioma. *J Clin Endocrinol Metab* 2004;89:3298-3305.

2. Ostrom QT, Gittleman H, Farah P, et al. CBTRUS statistical report: primary brain and central nervous system tumors diagnosed in the United States in 2006-2010. *Neuro Oncol* 2013;15(Suppl 2):ii1-56.

3. Osborn AG, Preece MT. Intracranial cysts: radiologic-pathologic correlation and imaging approach. *Radiology* 2006;239:650-664.

4. Muller HL, Gebhardt U, Faldum A, et al. Xanthogranuloma, Rathke's cyst, and childhood craniopharyngioma: results of prospective multinational studies of children and adolescents with rare sellar malformations. *J Clin Endocrinol Metab* 2012;97:3935-3943.

5. Harrison MJ, Morgello S, Post KD. Epithelial cystic lesions of the sellar and parasellar region: a continuum of ectodermal derivatives? *J Neurosurg* 1994;80:1018-1025.

6. Muller HL. Paediatrics: surgical strategy and quality of life in craniopharyngioma. *Nat Rev Endocrinol* 2013;9:447-449.

7. Garre ML, Cama A. Craniopharyngioma: modern concepts in pathogenesis and treatment. *Curr Opin Pediatr* 2007;19:471-479.

8. Cohen M, Guger S, Hamilton J. Long term sequelae of pediatric craniopharyngioma - literature review and 20 years of experience. *Front Endocrinol (Lausanne)* 2011;2:81.

9. Hamilton JK, Conwell LS, Syme C, Ahmet A, Jeffery A, Daneman D. Hypothalamic obesity following craniopharyngioma surgery: results of a pilot trial of combined diazoxide and metformin therapy. *Int J Pediatr Endocrinol* 2011;2011:417949.

10. Bereket A, Kiess W, Lustig RH, et al. Hypothalamic obesity in children. *Obes Rev* 2012;13:780-798.

11. Lustig RH. Hypothalamic obesity after craniopharyngioma: mechanisms, diagnosis, and treatment. *Front Endocrinol (Lausanne)* 2011;2:60.

12. Lustig RH, Hinds PS, Ringwald-Smith K, et al. Octreotide therapy of pediatric hypothalamic obesity: a double-blind, placebo-controlled trial. *J Clin Endocrinol Metab* 2003;88:2586-2592.

13. Danielsson P, Janson A, Norgren S, Marcus C. Impact sibutramine therapy in children with hypothalamic obesity or obesity with aggravating syndromes. *J Clin Endocrinol Metab* 2007;92:4101-4106.

14. Muller HL, Gebhardt U, Teske C, et al. Post-operative hypothalamic lesions and obesity in childhood craniopharyngioma: results of the multinational prospective trial KRANIOPHARYNGEOM 2000 after 3-year follow-up. *Eur J Endocrinol* 2011;165:17-24.

15. Elowe-Gruau E, Beltrand J, Brauner R, et al. Childhood craniopharyngioma: hypothalamus-sparing surgery decreases the risk of obesity. *J Clin Endocrinol Metab* 2013;98:2376-2382.

16. de Vile CJ, Grant DB, Hayward RD, Kendall BE, Neville BG, Stanhope R. Obesity in childhood craniopharyngioma: relation to post-operative hypothalamic damage shown by magnetic resonance imaging. *J Clin Endocrinol Metab* 1996;81:2734-2737.

17. Mai JK, Paxinos G, Voss T. Atlas of the human brain. San Diego, USA: Academic Press; 1997.

18. Wilke M, Holland SK, Altaye M, Gaser C. Template-O-Matic: a toolbox for creating customized pediatric templates. *Neuroimage* 2008;41:903-913.

19. Evans AC, Janke AL, Collins DL, Baillet S. Brain templates and atlases. *Neuroimage* 2012;62:911-922.

20. Baroncini M, Jissendi P, Balland E, et al. MRI atlas of the human hypothalamus. *Neuroimage* 2012;59:168-180.

21. Flegal KM, Cole TJ. Construction of LMS parameters for the Centers for Disease Control and Prevention 2000 growth charts. *Natl Health Stat Report* 2013:1-3.

22. Sorva R. Children with craniopharyngioma. Early growth failure and rapid postoperative weight gain. *Acta Paediatr Scand* 1988;77:587-592.

23. Muller HL, Heinrich M, Bueb K, et al. Perioperative dexamethasone treatment in childhood craniopharyngioma--influence on short-term and long-term weight gain. *Exp Clin Endocrinol Diabetes* 2003;111:330-334.

24. Van Gompel JJ, Nippoldt TB, Higgins DM, Meyer FB. Magnetic resonance imaging-graded hypothalamic compression in surgically treated adult craniopharyngiomas determining postoperative obesity. *Neurosurg Focus* 2010;28:E3.

25. Muller HL, Bueb K, Bartels U, et al. Obesity after childhood craniopharyngioma--German multicenter study on pre-operative risk factors and quality of life. *Klin Padiatr* 2001;213:244-249.

26. Puget S, Garnett M, Wray A, et al. Pediatric craniopharyngiomas: classification and treatment according to the degree of hypothalamic involvement. *J Neurosurg* 2007;106:3-12.

27. Roth CL, Gebhardt U, Muller HL. Appetite-regulating hormone changes in patients with craniopharyngioma. *Obesity (Silver Spring)* 2011;19:36-42.

28. Hochberg I, Hochberg Z. Expanding the definition of hypothalamic obesity. *Obes Rev* 2010;11:709-721.

29. Daousi C, Dunn AJ, Foy PM, MacFarlane IA, Pinkney JH. Endocrine and neuroanatomic features associated with weight gain and obesity in adult patients with hypothalamic damage. *Am J Med* 2005;118:45-50.

30. Vann SD. Re-evaluating the role of the mammillary bodies in memory. *Neuropsychologia* 2010;48:2316-2327.

31. Morton GJ, Cummings DE, Baskin DG, Barsh GS, Schwartz MW. Central nervous system control of food intake and body weight. *Nature* 2006;443:289-295.

32. Bouret SG, Draper SJ, Simerly RB. Trophic action of leptin on hypothalamic neurons that regulate feeding. *Science* 2004;304:108-110.

33. Glavas MM, Joachim SE, Draper SJ, Smith MS, Grove KL. Melanocortinergic activation by melanotan II inhibits feeding and increases uncoupling protein 1 messenger ribonucleic acid in the developing rat. *Endocrinology* 2007;148:3279-3287.

34. Mihaly E, Fekete C, Legradi G, Lechan RM. Hypothalamic dorsomedial nucleus neurons innervate thyrotropin-releasing hormone-synthesizing neurons in the paraventricular nucleus. *Brain Res* 2001;891:20-31.

35. van Swieten MM, Pandit R, Adan RA, van der Plasse G. The neuroanatomical function of leptin in the hypothalamus. *J Chem Neuroanat* 2014;61–62:207-220.

36. Harz KJ, Muller HL, Waldeck E, Pudel V, Roth C. Obesity in patients with craniopharyngioma: assessment of food intake and movement counts indicating physical activity. *J Clin Endocrinol Metab* 2003;88:5227-5231.

37. Holmer H, Pozarek G, Wirfalt E, et al. Reduced energy expenditure and impaired feeding-related signals but not high energy intake reinforces hypothalamic obesity in adults with childhood onset craniopharyngioma. *J Clin Endocrinol Metab* 2010;95:5395-5402.

38. Roth CL, Hunneman DH, Gebhardt U, Stoffel-Wagner B, Reinehr T, Muller HL. Reduced sympathetic metabolites in urine of obese patients with craniopharyngioma. *Pediatr Res* 2007;61:496-501.

39. Roth CL, Blevins JE, Ralston M, et al. A novel rodent model that mimics the metabolic sequelae of obese craniopharyngioma patients. *Pediatr Res* 2011;69:230-236.

40. Bingham NC, Rose SR, Inge TH. Bariatric surgery in hypothalamic obesity. *Front Endocrinol (Lausanne)* 2012;3:23.